

Thermal and economic optimization of an intercooler of three-stage compressor

Authors

Mahmood Mehregan^{a*}
Sayed Ehsan Alavi^b

^a Faculty of Mechanical Engineering, Shahrood University of Technology, Shahrood, Iran

^b Shohadaye Hoveizeh Campus of Technology, Shahid Chamran University of Ahvaz, Ahvaz, Iran

ABSTRACT

In this research, an intercooler of three-stage centrifugal compressor is investigated in order to decrease energy consumption. Due to the lack of comprehensive studies about optimization of efficiency and cost for the finned shell and tube intercoolers, with using non-dominated sorting genetic algorithm (NSGA-II), the efficiency of shell and tube heat exchanger with radial fin (intercooler) is studied to improve the performance of multi-stage compressor. The total cost and efficiency of an intercooler are selected as two objective functions. Also, some main decision variables, such as tube arrangement, mass flow rate on the tube and shell sides, the diameter of tubes, rate of tube pitch as well as inlet temperatures of tube and shell are considered. The heat transfer coefficients and the pressure drop of the shell-side are calculated based on Delaware modified method. The variation of efficiency based on the tube length, tubes number, baffle spacing ratio and tube pitch rate are investigated. The results show that using NSGA-II, the efficiency improves up to 96 %. Also, the best fins number per inch length of the tube is 26 which leads to the highest efficiency value. Results show that the tube shape has no effect on the efficiency and by increasing tube pitch rate the total costs decreases. The optimization results with NSGA-II is compared with the PSO method and it shows the accuracy of the genetic algorithm. Also, the thermal modeling is validated with another study and the maximum difference is estimated about 2%.

Article history:

Received : 19 August 2020

Accepted : 20 May 2021

Keywords: Shell and Tube Heat exchanger; Intercooler; Three-stage centrifugal compressor; Optimization; Genetic algorithm.

1. Introduction

The rise of the demand for energy and significant reductions in fossil fuels have increased the need to energy optimization. Since heat exchangers are widely used in the industry, reducing their energy losses is of great importance and many studies have been performed on this subject [1].

The study of the performance of intercoolers, in general, is done in two ways: the base of the first criterion is the first law of thermodynamics,

and the base of the second criterion is both of the first and second rules of thermodynamics. In heat exchangers, irreversibility occurs due to the limited temperature difference, fluid friction, and the mixing of the two liquids. Therefore, most studies in recent years have reduced the irreversibility of heat exchangers. Some of these studies are discussed below.

Amini et al. [2] studied the effect of two types of fin tubes on thermodynamic parameters in shell and tube heat exchangers using CFD results they showed that increasing fin pitch, decreases the efficiency.

* Corresponding author: Mahmood Mehregan
Faculty of Mechanical Engineering, Shahrood University of Technology, Shahrood, Iran
Email: chahartaghi@iust.ac.ir

Jia et al. [3] showed that in the fin-tube heat exchanger, the fins change the thickness of the thermal boundary layer and cause the interaction of velocity and temperature to be various at different pressures.

Arani et al. [4] used a numerical method to the thermo-hydraulic analysis of shell and tube heat exchanger. In this research they introduced a new type of baffle that decreases the energy and increases the lifetime of a heat exchanger.

Mohammadi et al. [5] using numerical analysis optimized the pressure drop and heat transfer of shell and tube heat exchanger with various porous baffles. Permeability, baffle cut and porosity are three parameters that are considered to obtain the optimum results.

Fares et al. [6] investigated the effect of nanofluid on the efficiency of shell and tube heat exchanger with experiments. The results showed that using 0.2% nanofluid of graphene/water, the heat transfer coefficient was enhanced by 29% .

Wang et al. [7] studied the effect of staggered baffles in the shell and tube heat exchangers. They also considered the heat transfer rate and pressure drop as two objective functions of their optimization. Using artificial neural networks they extracted the relationship between variable parameters and objective functions.

Bejan [8] studied the irreversibility of the heat exchangers in his study. The main reason for the irreversibility was two factors. The first is the conduction heat transfer and the second is fluid friction. The entropy generation resulting from this irreversibility was optimized in this research. The method of optimizing entropy generation is used in many thermodynamic systems that convert heat into work[9].

Guo et al.[10]introduced the concept of entransy dissipations. The entransy consist of two terms. Thermal term and friction term. The thermal term is due to limited temperature difference and the friction term is due to pressure drop. Results showed that entransy dissipations reduce heat transfer in irreversible systems and therefore they should be reduced.[11].

Venkata et al.[12] using Jaya algorithm optimized the shell and tube heat exchanger. The optimization results showed that the results

obtained from the Method Jaya algorithm are better than those of methods PSO and GA.

Chen and Ren [13]presented a new theory called minimizing thermal resistance theory to optimize the heat transfer rate in the process. Using a one-to-one correspondence between electrical concepts and thermal concepts they introduced a concept of general thermal resistance as a result of dividing the temperature difference into the heat flux.

Lemos et al. [14] optimized the shell and tube heat exchanger considering the fouling factor. The objective function of this study was to minimize the area of heat transfer or the total cost. In this research, an optimal heat exchanger using the linear method was designed.

Wen et al. [15] investigated the effect of helix angle on the shell and tube heat exchangers. They found that the maximum pressure drop occurs at an angle of 18 degrees. In this study, the average of overall heat transfer coefficient in the shell and tube heat exchanger increased by 28.3%.

Chahartaghi et al. [16] performed the optimal design of shell-and-tube heat exchangers by applying the entransy concept using genetic algorithm (GA) method. They investigated the performance improvement of heat exchanger with variations of some geometric parameters.

Mirzaei et al. [17]presented a multi-objective optimization using the genetic algorithm (GA) method for shell-and-tube heat exchangers. The thermal efficiency and cost of the system were considered as the objective functions. They utilized a method named constructal theory for the design of shell and tube heat exchanger and showed this technique could be proper for industrial applications in order of performance improvement of heat exchangers.

Abed et al.[18]introduced a new method for optimizing the shell and tube heat exchangers. Minimizing the total cost was the objective function, in this work. In the proposed algorithm, maximum pressure drop and geometric parameters are considered. It is found that the new method would significantly reduce the heat transfer area.

Lei et al. [19] used numerical simulations to design a louver baffles type of shell and tube heat exchanger and conventional segmental

baffles type. The comparisons of both types showed that, at similar conditions, conventional segmental baffles type of shell and tube heat exchanger requires higher pumping power.

Xu et al. [20, 21] found that the entransy dissipations in the shell and tube heat exchangers consist of two terms: friction term and thermal term. Also, they extracted that for optimizing the heat exchanger it is better to express this parameter in the form of dimensionless. It was also found that in the optimization of the shell and tube heat exchangers, the total number of entransy dissipations can be selected as the objective function.

Huang et al. [22] studied the effect of injected angle and velocity in a two-stage refrigerant compressor using numerical method. Results showed that increasing the injection angle, causes a significant increase in pressure drop in the intercooler.

Busaidi et al. [23] investigated the multistage industrial centrifugal compressors. They presented a new method for centrifugal compressors which can develop the compressor performance stage by stage.

Wu et al. [24] optimized the energy and cost in multi-stage compressors. The reduction of power compression, pumping power and the total costs of intercooler was the main goal of the research. In this study, each of the compressor stages was independently optimized.

Sathyaraj [25] compared CFD analysis and experimental data of intercooler. The circular cross-section pins are inserted normal to the flow direction of air in the existing finned tube heat exchanger (intercooler) of two-stage reciprocating air compressors to increase the convective surface contact area and create turbulence resulting in an increased heat transfer rate. The heat transfer rate has been increased in the modified intercooler to 10-22% of the existing intercooler. The outlet temperature of the intercooler has been reduced to 1.5%-2.5% of the inlet temperature in the modified intercooler. Modified intercooler has 1% - 1.5% efficient than existing.

Song et al. [26] introduced an empirical method to estimate the power consumption and the efficiency of multistage centrifugal compressors. The optimization technique was

applied to find an optimal strategy for compressed dry air systems. Results showed that about 5 % of power consumption was saved.

The multi optimization of the finned, shell, and tube heat exchanger has been performed in this study. With the help of MATLAB software [27], an optimization algorithm has been designed and implemented. In most of the previous studies, the heat transfer coefficient and the pressure drop on the shell side were extracted using Kern method, but this method is less accurate than the Simplified Delaware method. Thus, Simplified Delaware method has been used in this research. Also, in the past, there have been no studies about the optimization of efficiency and cost for the finned shell and tube intercoolers. In this research, an actual industrial case is studied. Besides that, an extensive analysis of the finned shell and tube heat exchanger has been presented. For this purpose, the effect of some variables including the number of fins per inch length of the tube, tube pitch rate, tube length, tube passes, the number of tubes, baffle spacing ratio, tube arrangement, tube shape on the efficiency and total cost have been investigated. Since, there has not been such a complete study so far, this study seems to be necessary and can be the complement of the previous works.

In summary, the most important research contributions can be described as follows:

- Thermal and economic modeling of finned shell and tube heat exchanger are presented.
- For thermal analysis, the heat transfer coefficients and the pressure drop of heat exchanger are evaluated with detail.
- The relationship between design parameters such as a number of fins per inch length of tube, tube pitch rate, tube arrangement, tube shape and efficiency have been analyzed.
- Impacts of design parameters such as the number of baffles, tube pitch rate, tube arrangement, tube shape on total cost have been investigated.
- Non-dominated sorting genetic algorithm is performed for optimization of intercooler of three-stage compressor

2. System description

The main Nitrogen compressor which is studied in this article is located in Fajr Petrochemical Company of Iran. The type of Subjected Compressor is a three-stage centrifugal compressor with two Intercoolers that are mounted between the stages and a cooler mounted after stage three. At first, the Nitrogen passes through inlet Nitrogen filter. The inlet Nitrogen filter consists of two high-efficiency filters and pre-filter pads. Compressed Nitrogen after leaving each stage, while passing through the intercoolers, is cooled by cooling water and enters the next stage of Compression. Types of intercoolers are shell and tube with a floating head. To avoid temperature increases, the Nitrogen is cooled twice while passing the compressor, between stage one and stage two and three. The case study compressor is shown in Fig.1.

3. Thermal modeling

In this study, longitudinal conduction heat transfer in the heat exchanger is neglected, also

potential and kinetic energy changes are not considered. The heat transfer loss between the intercooler and its environment is ignored [28], for the heat exchanger as shown in Fig.1, the equilibrium equation can be calculated as [28]:

$$\dot{Q} = (\dot{m}C_p)_h (T_{h,i} - T_{h,o}) = (\dot{m}C_p)_c (T_{c,o} - T_{c,i}) \quad (1)$$

In Eq. (1) C_p refers to the specific heat of the fluid at constant pressure, T is the temperature, \dot{Q} is the heat rate that has exchanged and \dot{m} represents the rate of mass flow. The indices o and i indicated the output and input of the intercooler, respectively. The indices of c and h , refer to a cold and hot fluid, respectively, and. The effectiveness of the intercooler is also can be expressed as follows [31]:

$$\varepsilon = \frac{2}{(1+c^*) + (1+c^{*2})^{0.5} \coth\left(\frac{NTU}{2}(1+c^{*2})^{0.5}\right)} \quad (2)$$

$$NTU = \frac{U_0 A_{tot}}{C_{min}} \quad (3)$$

$$C^* = \frac{C_{min}}{C_{max}} = \frac{\min((\dot{m}C_p)_s, (\dot{m}C_p)_t)}{\max((\dot{m}C_p)_s, (\dot{m}C_p)_t)} \quad (4)$$

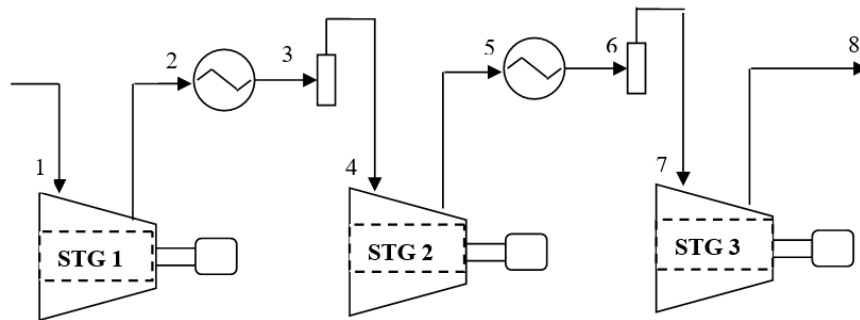


Fig.1: System Description

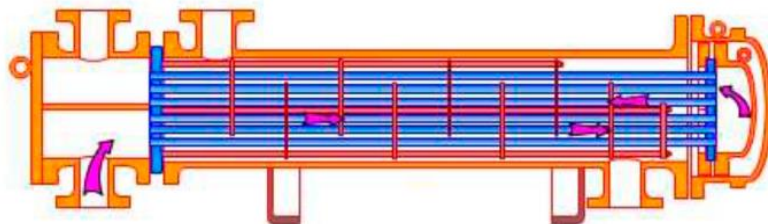


Fig.2. Shell and tube heat exchanger, type AES [29].

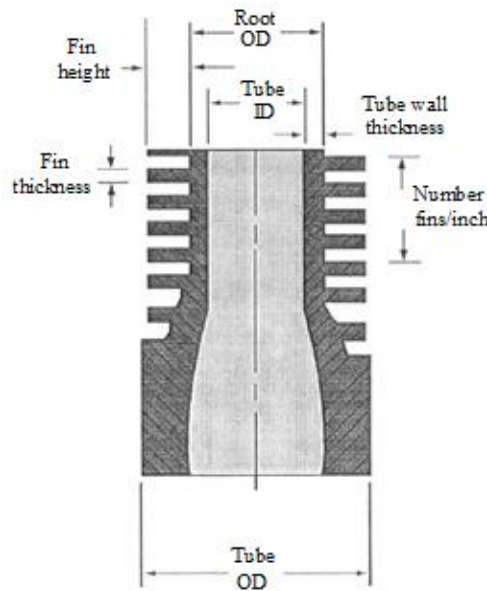


Fig.3. Radial low-fin tube[30].

Here NTU refers to the number of thermal units and dc^* indicates the rate of thermal capacity. U_0 is the overall heat transfer coefficient and A_{tot} refers to the total external surface area of the intercooler [30].

$$A_{tot} = A_{fins} + A_{prime} \quad (5)$$

$$A_{tot} = [2n_f \pi (r_{2c}^2 - r_1^2) + 2r_1 \pi (1 - n_f \tau)] L N_t \quad (6)$$

$$U_0 = \left[\frac{A_{tot}}{A_i h_i} + \frac{R_{Di} A_{tot}}{A_i} + \frac{A_{tot} \ln \frac{d_o}{d_i}}{2\pi K_{tube} L} + \frac{1}{h_o \eta_w} \frac{R_{Do}}{\eta_w} \right] \quad (7)$$

Here, $N_t, L, d_o, d_i, R_{Do}, R_{Di}, n_f, r_1, r_{2c}$ and K_w are tubes number, the length of the tube, tube outside diameter, tube inside diameter, fouling resistance of the shell side, fouling resistance of the tube side, fins number per unit length of the tube, root tube external radius, corrected fin radius and thermal conductivity of tube wall, respectively. Besides that, A_i is the internal surface area of the tube and can be expressed as [27, 29]:

$$A_i = \pi d_i L N_t \quad (8)$$

$$\eta_w = \left(\frac{A_{prime}}{A_{tot}} \right) + \eta_f \left(\frac{A_{fins}}{A_{tot}} \right) \quad (9)$$

$$\eta_f = \frac{\tanh(m\phi)}{(m\phi)} \quad (10)$$

$$\phi = (r_{2c} - r_1) \left[1 + 0.35 \ln \left(\frac{r_{2c}}{r_1} \right) \right] \quad (11)$$

$$m = \left(\frac{2h_o}{K\tau} \right)^{0.5} \quad (12)$$

$$r_{2c} = r_2 + \frac{\tau}{2} \quad (13)$$

where η_w refers to the weighted efficiency of the finned surface and η_f is the efficiency of fin. ϕ represents the efficiency of annular fins, and τ and K are the thickness of fin and thermal conductivity, respectively.

Using the following equation one can extract the coefficient of heat transfer on the tube-side [33-34]:

$$h_i = \left(\frac{k_t}{d_i} \right) 0.116 \left(Re_i^{2/3} - 125 \right) Pr_t^{1/3} \left(1 + \frac{d_i}{L} \right)^{1/4} \left(\frac{\mu}{\mu_w} \right)^{0.14} \quad \text{for } Re_i > 10^4 \quad (14)$$

$$h_i = \left(\frac{k_t}{d_i} \right) 0.027 Re_i^{0.8} Pr_t^{0.4} \left(\frac{\mu}{\mu_w} \right)^{0.14} \quad \text{for } 2100 < Re_i < 10^4$$

$$h_i = \left(\frac{k_t}{d_i} \right) 1.86 \left(\frac{Re_i Pr_t d_i}{L} \right)^{1/3} \left(\frac{\mu}{\mu_w} \right)^{0.14} \quad \text{for } Re_i < 2100$$

The above equation is acceptable for $\left(\frac{Re_i Pr_t d_i}{L} \right)^{1/3} \left(\frac{\mu}{\mu_w} \right)^{0.14} > 2$ and for $\left(\frac{Re_i Pr_t d_i}{L} \right)^{1/3} \left(\frac{\mu}{\mu_w} \right)^{0.14} < 2$ the

The coefficient of heat transfer on the tube-side can be calculated as follows [35]:

$$h_i = 3.66 \frac{k_t}{d_i} \quad (15)$$

Here, Pr_t, k_t, μ_w and μ refer to the Prandtl number on the tube side, thermal conduction coefficient of fluid on the tube side, the viscosity of fluid that has calculated at tube wall mean temperature and viscosity, respectively. The Reynolds number on the tube side can be expressed as following equation [30]:

$$Re_t = \frac{4\dot{m}_t \left(\frac{n_p}{N_t} \right)}{\pi d_i \mu} \quad (16)$$

where n_p and \dot{m}_t are tube passes number and the rate of mass flow, respectively.

Using the following equations the tube side pressure drop caused by fluid friction can be calculated [30, 36, 37]:

$$\Delta p_f = f \frac{L n_p}{2000 d_i} \frac{G_t^2}{s \left(\frac{\mu}{\mu_w} \right)^{0.14}} \quad (17)$$

$$G_t = \frac{4\dot{m}_t \left(\frac{n_p}{N_t} \right)}{\pi d_i^2} \quad (18)$$

$$f = \frac{64}{Re_t} \quad Re_t < 2300 \quad (19)$$

$$f = 0.4137 Re_t^{-0.2585} \quad Re_t > 2300$$

At the outlet and inlet of the tube there is a pressure drop that can be obtained from the following equation [30, 36, 37]:

$$\Delta p_r = 5 \times 10^{-4} \frac{\alpha_r G_t^2}{s} \quad (20)$$

α_r represents the velocity heads number used to calculate minor pressure drops on the tube-side, that extracts from Table 1 [30].

The pressure drop in the nozzle is given by the following equation [30, 36, 37]:

$$G_n = \frac{4\dot{m}_t}{\pi d_n^2} \quad (21)$$

$$Re_n = \frac{4\dot{m}_t}{\pi d_n \mu_t} \quad (22)$$

$$\Delta p_n = 7.5 \times 10^{-4} \frac{N_s G_n^2}{s} \quad \text{for turbulent flow} \quad (23)$$

$$\Delta p_n = 1.5 \times 10^{-3} \frac{N_s G_n^2}{s} \quad \text{for la minar flow}$$

where G_n refers to the mass flow that passes

through the nozzle, and N_s is the shells number that is located in series. Using the following equation the inner diameter of the shell can be obtained from [38]:

$$D_s = 0.637 p_T \sqrt{\pi N_s \frac{CL}{CTP}} \quad (24)$$

where CL is tube layout constant which equals 1 for 45° and 90° and 0.87 for 30° and 60°, p_T refers to the tube pitch. CTP is also estimated 0.9 for two pipe passes.

The heat transfer coefficient on the shell side, h_o , Using the Simplified Delaware method, is calculated [30, 33]:

$$h_o = j_H \left(\frac{K}{d_e} \right) Pr^{1/3} \left(\frac{\mu}{\mu_w} \right)^{0.14} \quad (25)$$

$$j_H = 0.5 \left(1 + \frac{B}{D_s} \right) \left(0.08 Re_s^{0.6821} + 0.7 Re_s^{0.1772} \right) \quad (26)$$

$$d_e = \frac{4p_T^2 - \pi d_r^2}{\pi d_r^*} \quad \text{for a square pitch} \quad (27)$$

$$d_e = \frac{4 \times 0.86 p_T^2 - \pi d_r^2}{\pi d_r^*} \quad \text{for atriangular pitch}$$

$$d_r^* = [d_r^2 + 4n_f \times b \times \tau (d_r + b)] \quad (28)$$

where j_H is the modified Colburn factor, d_e represents the equivalent diameter and b, d_r^*, d_r, τ and η_f are the height of fin, the effective root tube diameter, the external diameter of the root tube, the thickness of fin, the fins number per unit length of the tube, respectively.

The pressure drop on the shell side using the Simplified Delaware method is calculated as follow [33]:

$$\Delta p_s = \Delta p_{f,s} + \Delta p_n \quad (29)$$

$$\Delta p_{f,s} = \frac{f \times G_s^2 \times D_s \times (n_b + 1)}{2000 \times d_e \times s \times \left(\frac{\mu}{\mu_w} \right)^{0.14}} \quad (30)$$

where G_s is the shell side mass velocity and can be obtained as follow [30, 33]:

$$G_s = \frac{\dot{m}_s}{A_s} \quad (31)$$

$$A_s = \frac{D_s CB}{p_T} \quad (32)$$

where C refers to the clearance that there is between tubes in the bundles is the specific gravity of fluid, A_s represents flow area across

the tube bundle, n_b refers to the baffles number and Pr is the tube pitch.

The friction factor on the shell side is calculated from the following equation[30]:

$$f = 144 \left[f_1 - 1.25 \left(1 - \frac{B}{D_s} \right) (f_1 - f_2) \right] \quad (33)$$

$$f_1 = \exp \left[0.092 (\ln Re)^2 - 1.48 \ln Re - 0.000526 \left(\frac{D_s}{0.0254} \right)^2 + 0.0478 \frac{D_s}{0.0254} - 0.338 \right] \quad (35)$$

$$f_2 = \exp \left[0.123 (\ln Re)^2 - 1.78 \ln Re - 0.00132 \left(\frac{D_s}{0.0254} \right)^2 + 0.0678 \frac{D_s}{0.0254} - 1.34 \right]$$

Note that for $D_s > 0.59$ we take $D_s = 0.59$. The pressure drop on the shell-side nozzles can be calculated as the same way as the tube-side nozzles pressure drop.

The flowchart of the thermal modeling process has been presented in Fig. 4.

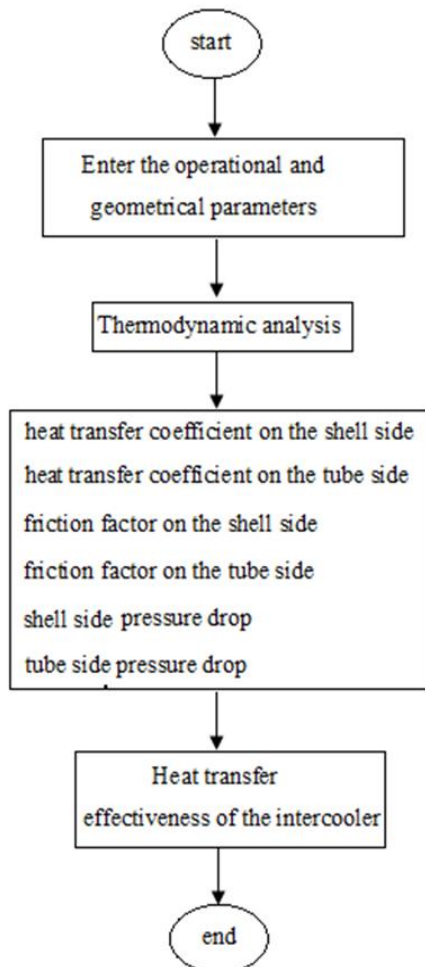


Fig.4: Flowchart of thermal modeling.

If $0.2032 \leq D_s \leq 0.59$ and $Re_t > 1000$:

$$f_1 = \left(0.0076 + 0.000166 \frac{D_s}{0.0254} \right) Re^{-0.125} \quad (34)$$

$$f_2 = \left(0.0016 + 5.8 \times 10^{-5} \frac{D_s}{0.0254} \right) Re^{-0.157}$$

If $0.2032 \leq D_s \leq 0.59$ and $Re_t < 1000$:

4. Multi-Objective Optimization using Genetic Algorithms

The operating costs including pumping to overcome frictional pressure loss and the capital cost for reducing the heat transfer surface are minimized in this research. The total cost equation consists of two terms. The term of operating cost and the term of initial capital cost. This equation can be written as follow [29]:

$$C_{total} = C_{in} + C_{op} \quad (36)$$

The initial capital cost C_{in} and the operating cost C_{op} for a shell and tube heat exchanger that the tube made of stainless steel can be obtained as following equations[29]:

$$P = \left(\frac{\dot{m}_t \Delta p_t}{\rho_t} + \frac{\dot{m}_s \Delta p_s}{\rho_s} \right) \times \frac{1}{\eta} \quad (37)$$

$$C_0 = P \times kel \times H \quad (38)$$

$$C_{op} = \sum_{k=1}^{ny} \frac{C_0}{(1+i)^k} \quad (39)$$

$$C_{in} = 8500 + 409A_{tot}^{0.85} \quad (40)$$

here C_o refers to the annual current cost, H represents the hours of operation per year, kel represents the unit price of electricity, i is the rate of annual inflation, ny is lifetime, P refers to pumping power and η is the efficiency of the pump. The total cost is selected as the objective function that should be minimized. The heat exchanger lifetime is considered to be $ny=10$ years; the rate of inflation is $i = 10\%$; the unit price of electrical energy is $kel = 0.15$ \$/kWh, the working hours is $H = 7500$ h/year and the

efficiency of the pump is $\eta = 0.6$, in this investigation. The total cost and efficiency of an intercooler are considered as two objective functions and improved the performance of the compressor. The thermophysical and process data for the intercooler designing is mentioned in Table 2.

The arrangement of the tube (30° , 45° , 90°), the fins number per unit length of the tube, and the diameter (among 23 available in the TEMA standard listed in Table 4) are three discrete optimization parameters [30]. The bounds for optimal design are mentioned in Table 3.

Table 2. The thermophysical properties for the intercooler

Parameter	Water (tube side)	Nitrogen (shell side)
Specific gravity (-)	0.99	0.97
Specific heat (J/kg K)	4190	1040
Dynamic viscosity (Pa s)	0.0007128	0.000021
Thermal conductivity (W/m K)	0.62	0.03
Fouling factor ($\text{m}^2\text{W/K}$)	0.00035	0.0004
Prandtl number (-)	4.82	0.72

Table 3. Bounds for optimal design.

Variable	Lower value	Upper value
Tube arrangement	(30° , 45° , 90°)	-
Rate of tube pitch	1.25	2
length of the tube (m)	3	8
Tube numbers	100	700
Ratio of baffle spacing	0.2	0.4
Thickness of fin (m)	0.000254	0.000304
Height of fin (m)	0.00127	0.003175
Fins Number per inch length of the tube	(16, 19, 26)	-
The inlet temperature of the tube ($^\circ\text{C}$)	15	35
The inlet temperature of the shell ($^\circ\text{C}$)	100	135
Mass flow rate on the tube side	8	20
Mass flow rate on the shell side	2	9

Table 4. Diameter of standard tubes (for radial low fin tubing):19 fins per tube inch).

	d_i (in)	d_o (in)	d_r (in)
1	0.29	0.5	0.37
2	0.38	0.63	0.50
3	0.46	0.75	0.63
4	0.58	0.88	0.75
5	0.71	1	0.87
6	0.28	0.5	0.37
7	0.36	0.63	0.50
8	0.49	0.75	0.62
9	0.56	0.88	0.75
10	0.69	1	0.87
11	0.26	0.5	0.37
12	0.53	0.75	0.62
13	0.63	0.88	0.75
14	0.76	1	0.87
15	0.66	1	0.87
16	0.37	0.63	0.50
17	0.51	0.75	0.62
18	0.62	0.88	0.75
19	0.74	1	0.87
20	0.40	0.63	0.50
21	0.48	0.75	0.62
22	0.61	0.88	0.75
23	0.73	1	0.87

The optimization of the intercooler is done by multi-objective Non-dominated Sorting Genetic Algorithm (NSGAI), in the present study. The maximum number of generations

and the size of the initial population are considered 200 and 100, respectively.

Figure 5 shows the flowchart of optimization procedure with algorithm genetic.

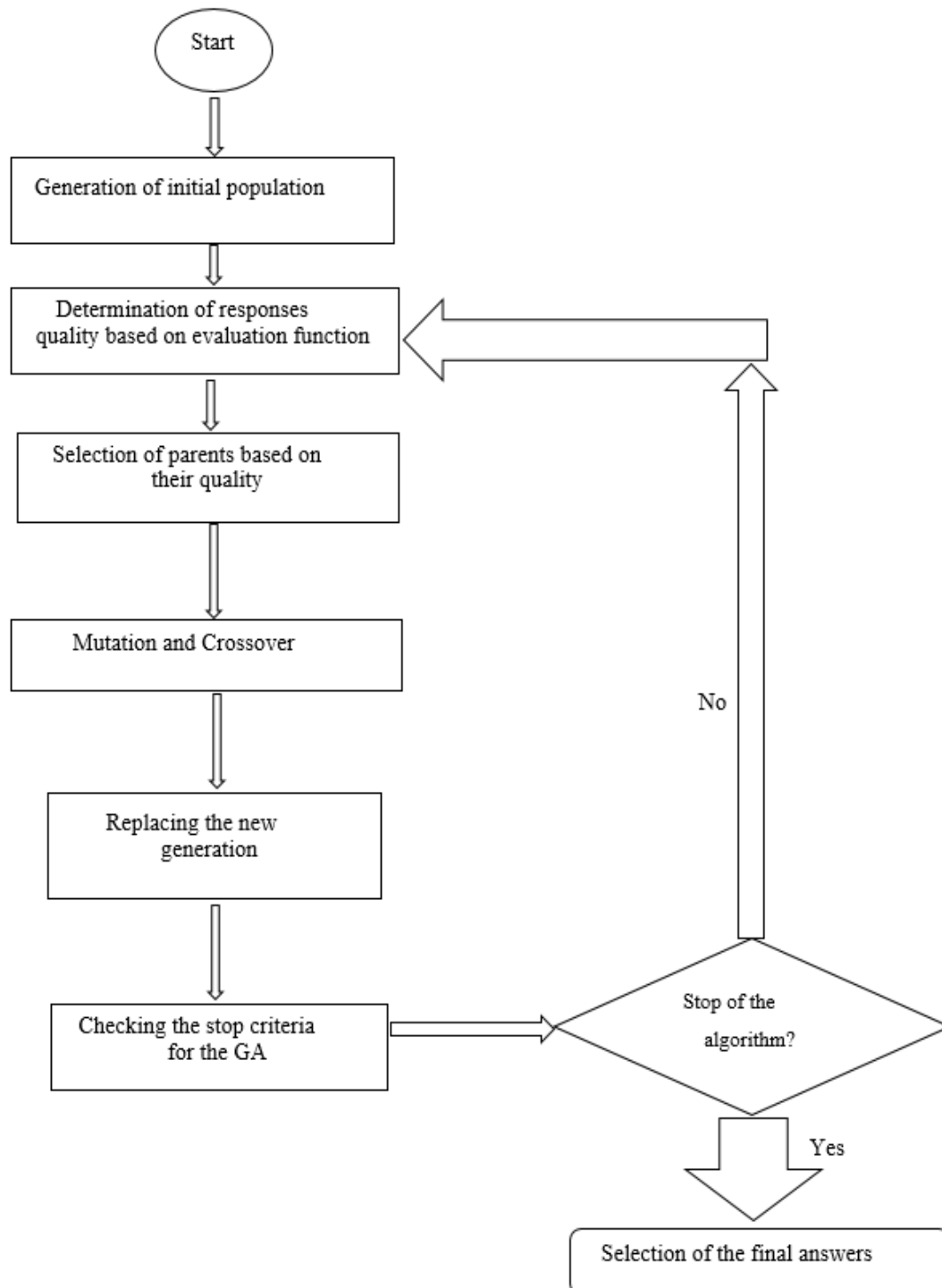


Fig.5: Flowchart of optimization model

5. Results and discussion

In this section, the result of the research has been presented. First validation of results has been analyzed about heat transfer properties according to Ref. [2].

Table 5 compares the results of this research with another study in a certain case of finned shell and tube heat exchanger. The results are in good agreement and the maximum difference in results is less than 2%.

Figure 6 shows the Pareto front, which represents the results of multi-objective optimization. The bounds of the efficiency for this optimization are between 58.2 % and 96 %. Fig.6 clearly shows that increased efficiency

will be associated with increased costs. So, based on the fact that which one is the main target of optimization, the three optimal designs are listed in Table 6. Point A shows the optimal design with the lowest cost. So, if the designer's goal is the lowest cost without regard to the value of efficiency, this case is recommended. Point B shows the optimal design with the highest efficiency at the highest cost. Therefore, if the designer's goal is the highest efficiency without regard to cost, this case is recommended. Point C represented an optimal design that delivers high efficiency at an affordable cost. Therefore, Point C located on the Pareto curve dominates compared to point A and Point B.

Table 5. Validation of results

Research	Efficiency (%)	Q(w)	h (W/m ² .K)
Present	31.963	97124	3016.28
Ref. [2]	31.90	96411	3069

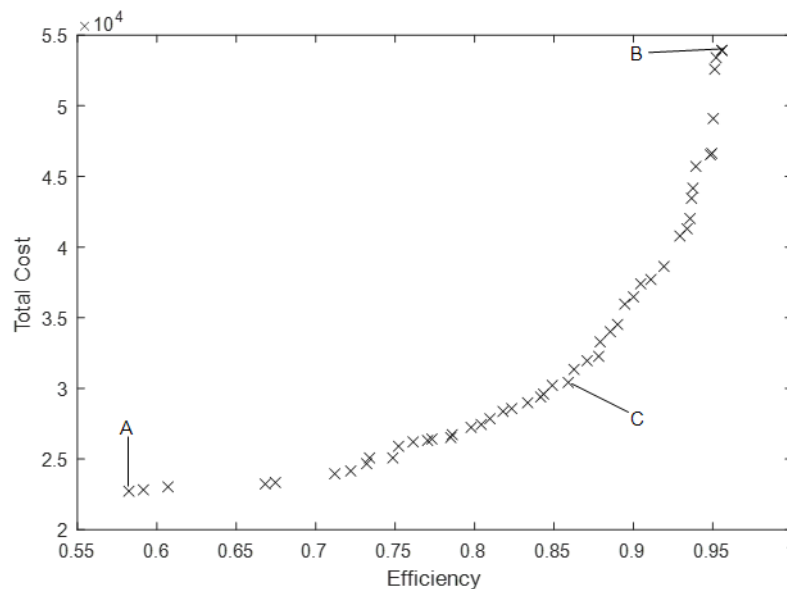


Fig.6. Optimized point's distribution in Pareto by using NSGA II.

Table 6. Choosing optimized points on the Pareto front.

Choice	Efficiency (%)	Total Cost (\$)
A	58.2	22710
B	96	53890
C	86	30430

In Table 7, to check the validity of the results, in a certain case in which total costs is chosen as a single objective function, the results of the genetic algorithms are compared with particle swarm optimization (PSO). As it is seen the results obtained from GA are in good agreement with the PSO algorithm.

Figure 7 shows the variation in the tube length on the efficiency. Because tube length has a direct relation to the NTU and Coth(NTU)

has an inverse relation to the efficiency, increasing this parameter, the efficiency increases. Results show that with an increase of 1 meter in tube length, the efficiency increases by about 5 %.It can be seen from Fig.8 that the lowest efficiency is the tube pass of 1 and the highest efficiency is the tube passes of 2. As a result, using a tube pass of 2 leads to the best design and highest efficiency.

Table 7. Comparison of results of methods GA and PSO

Specifications	Optimum (GA)	Optimum (PSO)
L	3	3.36
n_r	210	164
B	0.39	0.31
d_o	0.0222	0.0254
n_f	19	26
P	587.21	892
ΔP_s	53.14	65.66
ΔP_t	1450.8	5775
Total Costs (\$)	21963	25523.9

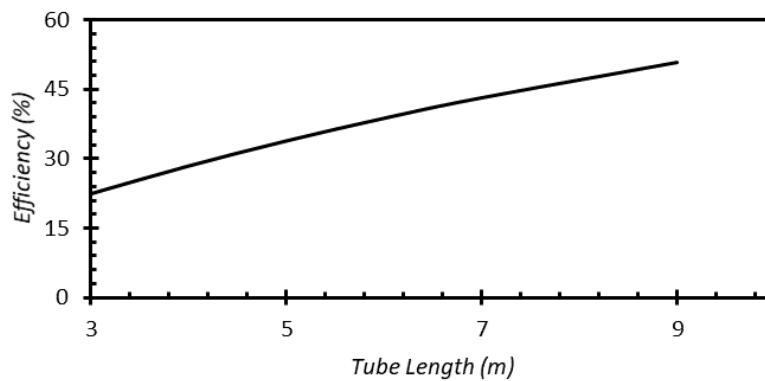


Fig.7. Variation of efficiency based on the tube length

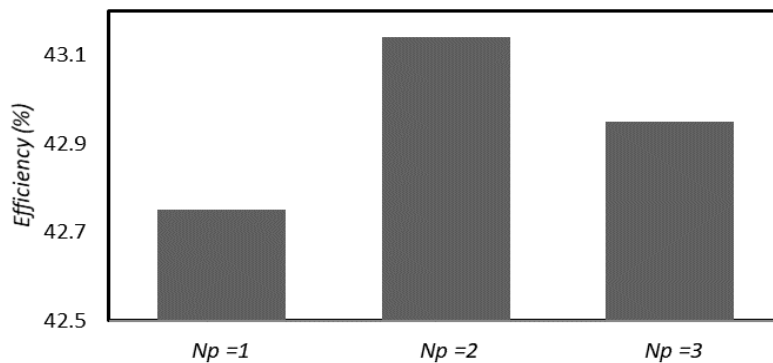


Fig.8. Comparison of tube passes

Figure 9 represents the effect of fins number per inch length of tube on the efficiency. As the NTU increases, the efficiency increases. Since increasing the fins number per inch length of the tube, increases the total area and total area has a direct relation to the NTU, it is found that by increasing this parameter, the efficiency increases. One can found from Fig. 10 that tube shape has no effect on efficiency. This result seems logical as the tube shape affects the pressure drop slightly.

Fig. 11 represents the effect of the number of the tubes on the efficiency. On the one hand, the

number of the tubes has a direct relation to the area, and on the other hand, area has a direct relation to the NTU, increasing this parameter, the efficiency increases. As the number of tubes increases from 100 to 500, the efficiency increases significantly and with increasing of more than 500 tubes, the efficiency increases slightly. It can be seen from Fig. 12 that the lowest efficiency is the tube arrangement of 45° and the highest efficiency is the tube arrangement of 30° . As a result, using a tube arrangement of 30° leads to the best design and highest efficiency.

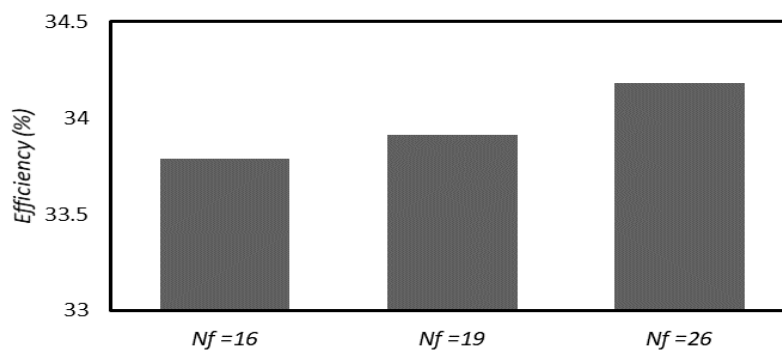


Fig.9. Comparison of the number of fins per inch length of tube

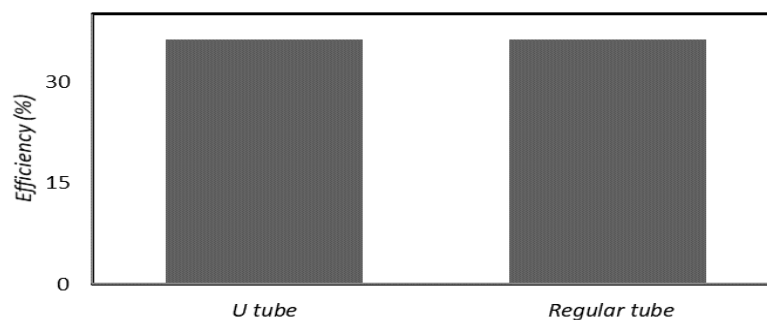


Fig.10. Comparison of the tube shape

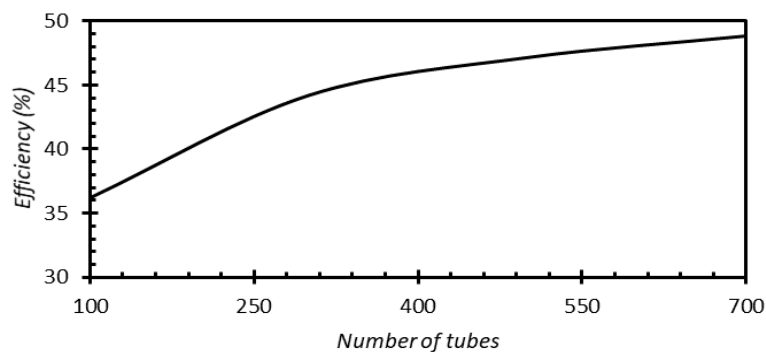


Fig.11. Variation of efficiency based on the tubes number

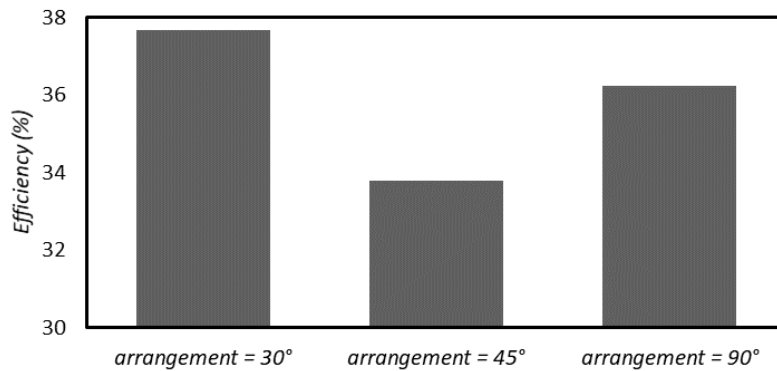


Fig.12. Comparison of the tube arrangement

Figure 13 and Fig. 14 show the effect of the baffle spacing ratio and tube pitch rate on the efficiency. As the overall heat transfer coefficient increases, the NTU increases. Since overall heat transfer coefficient has an inverse relation to the baffle spacing ratio and tube pitch rate. It is found that by increasing these

parameters, the efficiency decreases. Results show that with an increase of 0.1 in baffle spacing ratio, the efficiency decreases by about 1.2 %. Also, it is found that with an increase of 0.1 in tube pitch rate, the efficiency decreases by about 5.3 %.

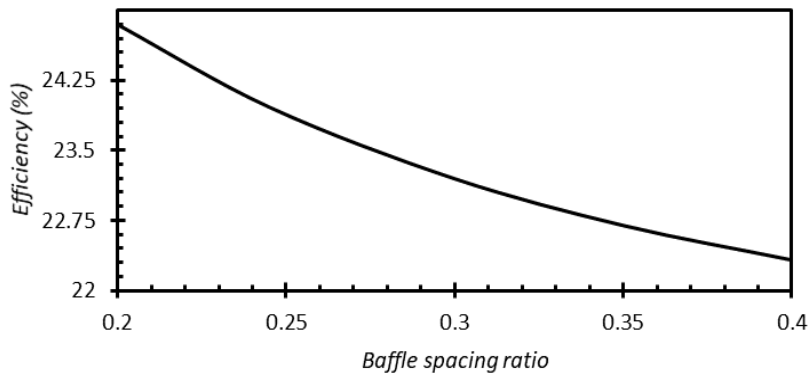


Fig.13. Variation of efficiency based on the baffle spacing ratio.

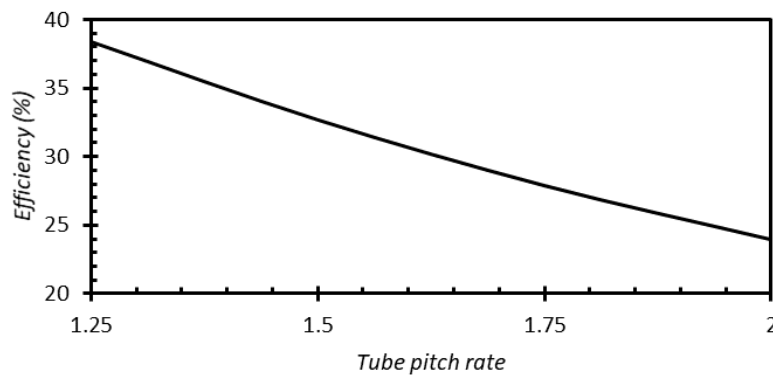


Fig.14. Variation of efficiency based on the tube pitch rate.

Figure 15 and Fig. 16 show, the changes in the total costs of the heat exchanger in terms of the shell side pressure drop and mass flow rate on the tube side under constant heat transfer rate conditions. Due to the fact that the total costs have a direct relation to the shell side pressure drop and mass flow rate on the tube side. As can be seen from these figures, by increasing these parameters, the total cost of the heat exchanger increases.

Figure 17 and Fig. 18 show the variation in the number of baffles in the shell on the pressure drop and total costs in the conditions of the constant heat transfer rate. Physically, the pressure drop increases as the number of baffles increases. Since the pressure drop has a direct relation to the total costs, by decreasing this parameter the total costs decreases.

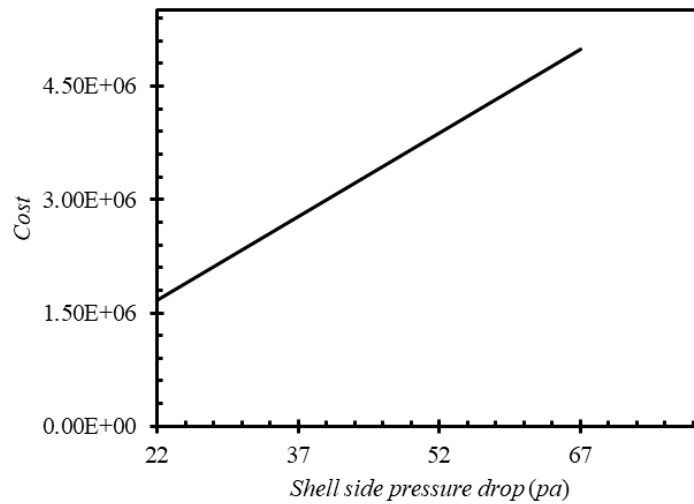


Fig. 15. Variation of total costs (in dollars) based on the shell side pressure drop

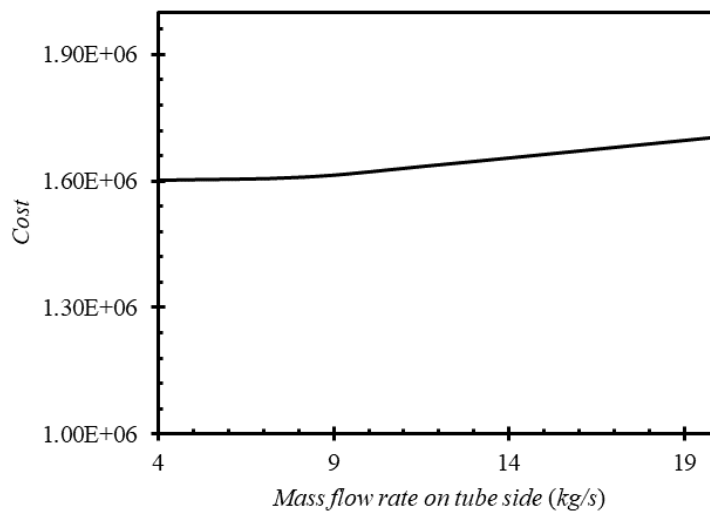


Fig. 16. Variation of total costs (in dollars) based on the mass flow rate on tube side

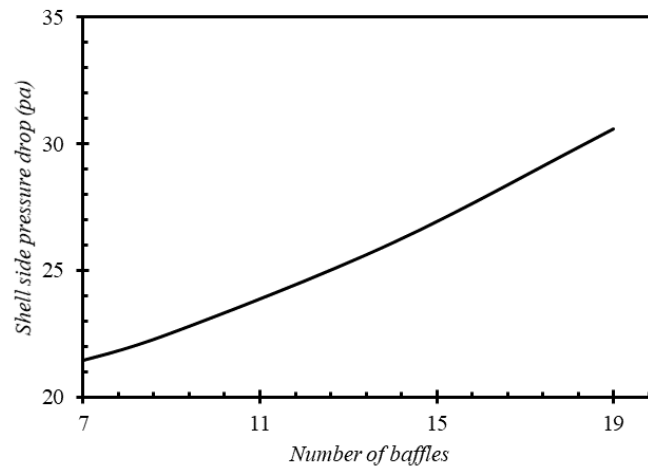


Fig. 17. Variations of shell side pressure drop with the number of baffles.

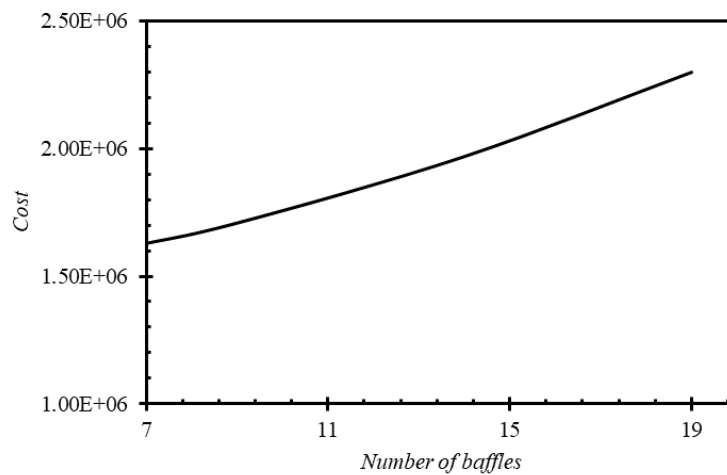


Fig. 18. Variations of total costs (in dollars) with the number of baffles

Figure 19 and Fig. 20 show the variation in the tube pitch rate on the pressure drop and total costs in the conditions of the constant heat transfer rate. Physically, the pressure drop decreases as the tube pitch rate increases. Because the pressure drop has a direct relation to the total costs, by increasing tube pitch rate the total costs decreases.

The variations of total costs with the tube arrangement have been presented in Table 8.

Table 8. Variations of total costs with the tube arrangement.

arrangement	Δps	cost
30	24.13468	1.83E+06
45	21.18727	1.61E+06
90	22.90878	1.74E+06

It can be seen from Table 8 that the lowest pressure drop and costs belong to the tube arrangement of 45° and the highest pressure drop and costs are belong to the tube arrangement of 30°. Results show that using a tube arrangement of 45° compared to 30°, 12% the total cost is reduced. It can be found from Table 9 that U-tubes have lower pressure drop and costs compared to regular tubes. Results show that using U-tubes, the total cost is reduced by about 577.5 \$.

Table 9. Variations of total costs with the tube shape.

Tube shape	Δpt	cost
Regular	88.77538	1608896.2
U-type	82.67884	1608318.7

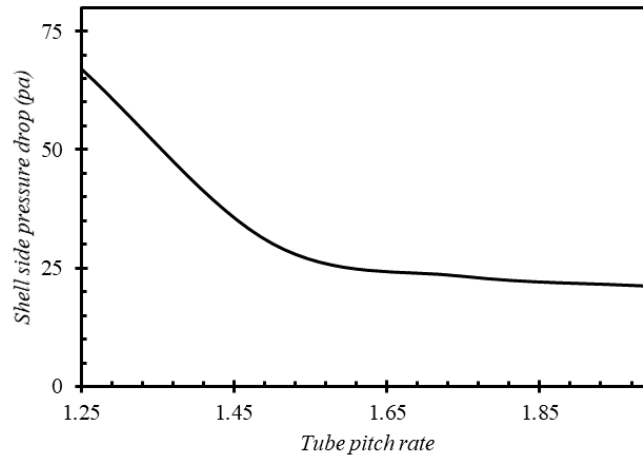


Fig. 19. Variations of pressure drop with the tube pitch rate.

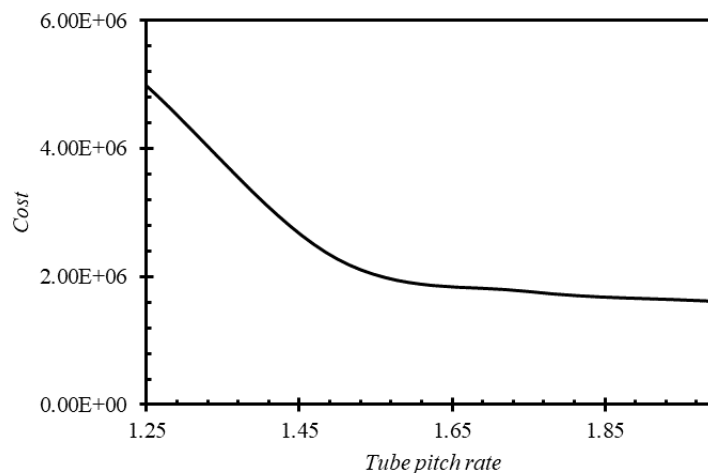


Fig. 20. Variations of total costs (in dollars) with the tube pitch rate

6. Conclusion

In this research, an actual industrial intercooler of a three-stage centrifugal compressor has been modeled and achieved to better performance the system have been optimized from energy and economic issues. The efficiency and total cost has been selected as two objective functions and multi-objective optimization method has been presented. The objective functions have been optimized based on main variables including the tubes number, the diameter of the tube, the length of the tube, the height of fin, the thickness of fin, the fins number per inch length of the tube, and the ratio of baffle spacing. Three points on the Pareto front are recommended as optimal points. In this study, the lowest of total

cost and the highest of efficiency is developed 22710 \$ and 96 % respectively. The key results of this research can be summarized as below:

- Results show that increasing the tube length or number of tubes, increases the efficiency.
- Results indicate that decreasing the baffle spacing ratio of tube pitch rate, leads to rise of the efficiency increases.
- The best tube arrangement has the highest value of efficiency tube arrangement of 30°.
- The best tube passes number which has the highest value of efficiency tube passes of 2.

- The best fins number per inch length of the tube which has the highest value of efficiency is fins number per inch length of tube of 26.
- Results show that the tube shape has no effect on efficiency.
- Total costs will increase under the effect of increasing pressure drop and mass flow rate.
- Total costs will increase under the effect of increasing the number of baffles.
- Total costs will decrease under the effect of increasing the tube pitch ratio.
- Total costs have the lowest value using tube arrangement of 45°.
- Total costs were reduced by using U-tubes instead of regular tubes.
- Results show that the genetic algorithm method of optimization is in good agreement with the PSO method.

7. References

- [1] M. Longeon, S. Adèle, F. Jean-François, B. Arnaud and M. Philippe, Experimental and numerical study of annular PCM storage in the presence of natural convection, *Applied energy* 112 (2013): 175-184.
- [2] R.Amini, et al. "Numerical investigation on effects of using segmented and helical tube fins on thermal performance and efficiency of a shell and tube heat exchanger." *Applied Thermal Engineering* 138 (2018): 750-760.
- [3] R.Z. Jia, Y.C. Wang, J. Guo, Z.Y. Yu, H.F. Kang, Research on the heat transfer and flow characteristics of fin-tube exchanger under low pressure environment, *Applied Thermal Engineering* 112(2017) 1163-1171.
- [4] A.A. Arani and R. Moradi, Shell and tube heat exchanger optimization using new baffle and tube configuration, *Applied Thermal Engineering*, 157 (2019), 113736.
- [5] M. H. Mohammadi, H. R. Abbasi, A. Yavarinasab, H. Pourrahmani, Thermal optimization of shell and tube heat exchanger using porous baffles, *Applied Thermal Engineering*, 170, (2020), 115005. <https://doi.org/10.1016/j.applthermaleng.2020.115005>.
- [6] M. Fares, M. AL-Mayyahi, M. AL-Saad, Heat transfer analysis of a shell and tube heat exchanger operated with graphene nanofluids, *Case Studies in Thermal Engineering*, 18 (2020), 100584.
- [7] X. Wang, N. Zheng, Z. Liu, W. Liu, Numerical analysis and optimization study on shell-side performances of a shell and tube heat exchanger with staggered baffles, *International Journal of Heat and Mass Transfer*. 124 (2018), 247–259.
- [8] A. Bejan, 1982, *Entropy Generation Through Heat and Fluid Flow*.
- [9] J. E. Hesselgreaves, Rationalisation of second law analysis of heat exchangers, *International Journal of Heat and Mass Transfer*, Vol. 43, No. 22, pp. 4189-4204, 2000/11/15/, 2000.
- [10] Z.-Y. Guo, H.-Y. Zhu, X.-G. Liang, Entransy—a physical quantity describing heat transfer ability, *International Journal of Heat and Mass Transfer*, Vol. 50, No. 13-14, pp. 2545-2556, 2007.
- [11] G.-Z. Han, Z.-Y. Guo, Physical mechanism of heat conduction ability dissipation and its analytical expression, in *Proceeding of*, 98-102.
- [12] R. V. Rao, A. Saroj, Economic optimization of shell-and-tube heat exchanger using Jaya algorithm with maintenance consideration, *Applied Thermal Engineering*, Vol. 116, pp. 473-487, 2017.
- [13] Q. Chen, J. Ren, Generalized thermal resistance for convective heat transfer and its relation to entransy dissipation, *Chinese Science Bulletin*, Vol. 53, No. 23, pp. 3753-3761, 2008.
- [14] J. C. Lemos, A. L. Costa, M. J. Bagajewicz, Linear method for the design of shell and tube heat exchangers including fouling modeling, *Applied Thermal Engineering*, Vol. 125, pp. 1345-1353, 2017.
- [15] J. Wen, X. Gu, M. Wang, S. Wang, S. Tu, Numerical investigation on the multi-objective optimization of a shell and tube heat exchanger with helical baffles, *International Communications in Heat and Mass Transfer*, Vol. 89, pp. 91-97, 2017.
- [16] M. Chahartaghi, P. Eslami, A. Naminezhad, Effectiveness improvement and optimization of shell-and-tube

- heat exchanger with entransy method, *Heat and Mass Transfer*, Vol. 54, No. 12, pp 3771–3784, 2018.
- [17] M. Mirzaei, H. Hajabdollahi, H. Fadakar, Multi-objective optimization of shell-and-tube heat exchanger by constructal theory, *Applied Thermal Engineering*, Vol. 125, pp. 9-19, 2017/10/01/, 2017.
- [18] A. M. Abed, I. A. Abed, H. S. Majdi, A. N. Al-Shamani, K. Sopian, A new optimization approach for shell and tube heat exchangers by using electromagnetism-like algorithm (EM), *Heat and Mass Transfer*, Vol. 52, No. 12, pp. 2621-2634, 2016.
- [19] Y. Lei, Y. Li, S. Jing, C. Song, Y. Lyu, F. Wang, Design and performance analysis of the novel shell-and-tube heat exchangers with louver baffles, *Applied Thermal Engineering*, Vol. 125, pp. 870-879, 2017.
- [20] M. Xu, L. Cheng, J. Guo, An application of entransy dissipation theory to heat exchanger design, *Journal of Engineering Thermophysics*, Vol. 30, No. 12, pp. 2090-2092, 2009.
- [21] M. Xu, J. Guo, L. Cheng, Application of entransy dissipation theory in heat convection, *Frontiers of Energy and Power Engineering in China*, Vol. 3, No. 4, pp. 402, 2009.
- [22] J.-M. Huang, C.-P. Chiang, J.-F. Chen, Y.-L. Chow, C.-C. Wang, Numerical investigation of the intercooler of a two-stage refrigerant compressor, *Applied thermal engineering*, Vol. 27, No. 14-15, pp. 2536-2548, 2007.
- [23] W. Al-Busaidi, P. Pilidis, A new method for reliable performance prediction of multi-stage industrial centrifugal compressors based on stage stacking technique: Part I—existing models evaluation, *Applied Thermal Engineering*, Vol. 98, pp. 10-28, 2016.
- [24] Y. Wu, J. Hamilton, W. Shenghong, Optimization of shell-and-tube intercooler in multistage compressor system, 1982.
- [25] A. Sathyaraj, Analysis and performance enhancement of intercooler in two stage reciprocating air compressor using CFD, *International Journal of Application in Mechanical and Production Engineering*, Vol. 1, pp. 1-5, 2015.
- [26] K. Song, C. Jeong, C. Han, Hybrid Compressor Model for Optimal Operation of CDA System, in: *Computer Aided Chemical Engineering*, Eds., pp. 889-894: Elsevier, 2010.
- [27] W. Gander, Starting and Using Matlab, in: *Learning MATLAB*, Eds., pp. 1-9: Springer, 2015.
- [28] R. K. Shah, D. P. Sekulic, 2003, *Fundamentals of heat exchanger design*, John Wiley & Sons,
- [29] H. Sadeghzadeh, M. Aliehyaei, M. A. Rosen, Optimization of a Finned Shell and Tube Heat Exchanger Using a Multi-Objective Optimization Genetic Algorithm, *Sustainability*, Vol. 7, No. 9, pp. 11679-11695, 2015.
- [30] R. W. Serth, T. Lestina, 2014, *Process heat transfer: Principles, applications and rules of thumb*, Academic Press,
- [31] S. Kakac, H. Liu, A. Pramuanjaroenkij, 2012, *Heat exchangers: selection, rating, and thermal design*, CRC press,
- [32] F. McQuiston, D. Tree, Optimum space envelopes of the finned tube heat transfer surface, *ASHRAE Trans*, 78(2), (1972),, 144-152.
- [33] D. Kern, A. Kraus, *Extended Surface Heat Transfer*, McGraw-Hill, New York, 1972.
- [34] H. Hausen, Darstellung des Wärmeüberganges in Rohren durch verallgemeinerte Potenzbeziehungen, *Z. VDI Beih. Verfahrenstech*, Vol. 4, pp. 91-98, 1943.
- [35] E. N. Sieder, G. E. Tate, Heat transfer and pressure drop of liquids in tubes, *Industrial & Engineering Chemistry*, Vol. 28, No. 12, pp. 1429-1435, 1936.
- [36] D. Q. Kern, 1950, *Process heat transfer*, Tata McGraw-Hill Education,
- [37] J. Henry, Headers, nozzles, and turnarounds, *Heat Exchanger Design Handbook*, Vol. 2, 1982.
- [38] J. Taborek, 1991, *Industrial heat exchanger design practice*, Wiley, New York.